Optimal Partitioning for Multi-Vehicle Systems Using Quadratic Performance Criteria ⋆

Efstathios Bakolas [a]

[a] *Department of Aerospace Engineering and Engineering Mechanics, The University of Texas at Austin, Austin, Texas 78712-1221, USA*

Abstract

We consider the problem of characterizing a generalized Voronoi diagram that is relevant to a special class of area assignment problems for multi-vehicle systems. It is assumed that the motion of each vehicle is described by a second order mechanical system with time-varying linear or affine dynamics. The proposed generalized Voronoi diagram encodes information regarding the proximity relations between the vehicles and arbitrary target points in the plane. These proximity relations are induced by an anisotropic (generalized) distance function that incorporates the vehicle dynamics. In particular, the generalized distance is taken to be the minimum square integral control associated with the transition of a vehicle to an arbitrary target point with a small terminal velocity at a fixed final time. The space we wish to partition corresponds to the union of all the terminal positions that can be attained by each vehicle using finite control effort. Consequently, the partition space has lower dimension than the state space of each vehicle. We show that, in the general case, the solution to the proposed partitioning problem can be associated with a power Voronoi diagram generated by a set of spheres in a five-dimensional Euclidean space for the computation of which efficient techniques exist in the relevant literature.

Key words: Autonomous agents, Voronoi diagrams, spatial partitioning, multi-vehicle systems, computational methods.

1 Introduction

We consider a generalized Voronoi partitioning problem whose solution is purport to encode information relevant to *area assignment* problems [1] involving multi-vehicle systems. A typical example would be the following: Let us assume that a service request for on site service is issued at some point in the vicinity of a team of vehicles. Which vehicle should respond to this request? A standard approach for addressing this type of problems would be the following. First, compute a Voronoi diagram encoding the necessary information about the proximity relations between the vehicles and arbitrary points in the plane based on their relative Euclidean distances. Subsequently, assign the task to the vehicle that is closer to the point where the service request was issued than any other vehicle from the same team. The main caveat of the previous approach has to do with the fact that the Euclidean distance is not always the most appropriate figure of merit for characterizing the proximity relations between the vehicles and arbitrary points in the plane. This is because the Euclidean distance does not encode any information regarding, for example, neither the initial velocities nor the dynamics of the vehicles.

Standard Voronoi diagrams generated by a finite point-set (set of generators), whose proximity metric is the Euclidean distance, and multiplicative (additive) weighted Voronoi diagrams, whose proximity metric is, in turn, the product (respectively, the sum) of the Euclidean distance with a different positive weight assigned to each generator, and their variations [2–4], have been extensively used in applications of autonomous agents ranging from vehicle routing [5–7] to coverage problems [8–11], just to name a few. Another important class of generalized Voronoi diagrams are the so-called *anisotropic* Voronoi diagrams [12], which find applications in coverage problems involving anisotropic (that is, direction dependent) sensors [13]. In contradistinction with the multiplicative weighted Voronoi diagram, the (possibly different) weights assigned to each generator of an anisotropic Voronoi diagram are positive definite matrices rather than positive scalars. The "anisotropic" qualifier for this class of generalized Voronoi diagrams stems from the fact that the weighting matrices assigned to each generator may not, in general, uniformly weigh the proximity distance function along different directions.

⋆ Corresponding author E. Bakolas. Tel.: +1 512 471 4250;
Email address: bakolas@austin.utexas.edu (Efstathios Bakolas).

Typically, the choice of the proximity metric of the generalized Voronoi partitions utilized in problems involving multiple agents, as the ones previously mentioned, stems from geometric considerations relevant to the following question: "which agent is the closest to the target?" In our previous work [14–16], which was initially motivated by the work presented in [17,18], we have highlighted the potential of using a different class of generalized Voronoi diagrams with respect to standard system / control theoretic "metrics" in problems of multi-vehicle systems. In this framework, one is interested in addressing questions like: "which vehicle can reach a target with minimum transition cost?" Typical examples of this new class of proximity metrics, to which we refer as *state-dependent* metrics [15], are the minimum time of arrival, control effort and fuel to-go. It is important to note that these pseudo-metrics are not, in general, only functions of the initial and terminal points but the whole trajectory that connects them as well. Consequently, state-dependent metrics are anisotropic functions which cannot, in general, be directly associated with the classes of generalized Voronoi diagrams for which efficient computational techniques are available. In contradistinction with [14,15], which focus on state-dependent metrics for vehicles with single integrator type kinematics, in this work, we consider multi-vehicle systems with second order, time-varying linear or affine dynamics. The space we wish to partition, the *partition space*, consists of all the points in the plane that can be reached by any vehicle from the team with a small terminal speed. Consequently, the partition space is a space of positions, and as such has lower dimension than the state space of each vehicle, which is a space of both positions and velocities. In addition, the proximity metric is a standard quadratic performance criterion from linear optimal control, namely the minimum (weighted) integral square control, also known as the minimum (weighted) *control effort* [19,20].

Next, we summarize the main contributions of this work. First, we propose an area assignment problem [1] with respect to an anisotropic, state-dependent proximity metric, namely the minimum control effort, for a multi-vehicle system with second order dynamics and frame the problem as a generalized Voronoi diagram problem. To the best of the author's knowledge, this is the first attempt to address this class of partitioning problems in the literature. Second, we demonstrate that the solution to this new class of generalized Voronoi diagram problems can be reduced to the construction of generalized Voronoi diagrams for the computation of which efficient algorithms exist in the literature of computational geometry. In particular, we show that, when the vehicles do not necessarily have identical transition cost functions, the solution to the partitioning problem can be obtained by the projection of a power Voronoi diagram generated by a set of spheres embedded in a five-dimensional Euclidean space on the two-dimensional partition space. In the case when all the vehicles have the same transition cost function, the solution to the proposed partitioning problem reduces to the computation of an affine Voronoi diagram, which is associated, in turn, with a power Voronoi diagram generated by a set of circles. These important results have allowed us to characterize modest bounds on the time required to compute the proposed spatial partitions as well as their combinatorial complexity [1] , which confirm the practicality of employing the proposed class of spatial partitions in applications of multi-vehicle systems.

The rest of the paper is organized as follows. Section 2 presents the formulation of the optimal control problem for a single vehicle. The partitioning problem for the multi-vehicle scenario is formulated and subsequently addressed in Sections 3 and 4, respectively. Section 5 presents simulation results, and finally, Section 6 concludes the paper with a summary of remarks.

2 Formulation of the Optimal Steering Problem

We are given a team of n vehicles which are located at n distinct points $\bar{\mathsf{x}}_i \in \mathbb{R}^2$ with prescribed initial velocities $\bar{\mathsf{v}}_i \in \mathbb{R}^2$, where $i \in \mathcal{I}_n := \{1, \ldots, n\}$. We denote by $\overline{\mathcal{X}} := \{\bar{\mathsf{x}}_i \in \mathbb{R}^2 : \ i \in \mathcal{I}_n\}$ and $\overline{\mathcal{V}} := \{\bar{\mathsf{v}}_i \in \mathbb{R}^2 : \ i \in \mathcal{I}_n\}$, respectively, the sets comprised of the initial positions and velocities of the vehicles. The motion of the i-th vehicle from the team, where $i \in \mathcal{I}_n$, is described by the following set of equations

$$\begin{aligned} \dot{\mathsf{x}}_i &= \mathsf{v}_i, & \mathsf{x}_i(0) &= \bar{\mathsf{x}}_i, \\ \dot{\mathsf{v}}_i &= \mathbf{G}_i(t)\mathsf{v}_i + \mathbf{H}_i(t)u_i(t) + f_i(t), & \mathsf{v}_i(0) &= \bar{\mathsf{v}}_i, \end{aligned} \quad (1)$$

where $\mathsf{x}_i := [x_i, \ y_i]^{\mathrm{T}} \in \mathbb{R}^2$ ($\bar{\mathsf{x}}_i := [\bar{x}_i, \ \bar{y}_i]^{\mathrm{T}} \in \mathbb{R}^2$) and $\mathsf{v}_i := [v_i, \ w_i]^{\mathrm{T}} \in \mathbb{R}^2$ ($\bar{\mathsf{v}}_i := [\bar{v}_i, \ \bar{w}_i]^{\mathrm{T}} \in \mathbb{R}^2$) are, respectively, the position and velocity vectors of the i-th vehicle at time t (at time $t = 0$). For a given velocity vector $\mathsf{v}_i^\star = [v_i^\star, \ w_i^\star]^{\mathrm{T}} \in \mathbb{R}^2$, we define the *position space* to be the hyperplane $\mathcal{X}(\mathsf{v}_i^\star) := \{[\mathsf{x}_i^{\mathrm{T}}, \ (\mathsf{v}_i^\star)^{\mathrm{T}}]^{\mathrm{T}} : \ \mathsf{x}_i \in \mathbb{R}^2\}$. Furthermore, we will denote the state vector of the i-th vehicle at time $t = 0$ and time t by z_i and $\bar{\mathsf{z}}_i$, respectively, where $\mathsf{z}_i := [\mathsf{x}_i^{\mathrm{T}}, \ \mathsf{v}_i^{\mathrm{T}}]^{\mathrm{T}}$ and $\bar{\mathsf{z}}_i := [\bar{\mathsf{x}}_i^{\mathrm{T}}, \ \bar{\mathsf{v}}_i^{\mathrm{T}}]^{\mathrm{T}}$. In addition, $u_i(\cdot) \in \mathcal{L}^2([0, T_{\mathsf{f}}], \mathbb{R}^2)$ is the control input of the i-th vehicle, where $\mathcal{L}^2([0, T_{\mathsf{f}}], \mathbb{R}^2)$ denotes the space of square integrable functions $g : [0, T_{\mathsf{f}}] \mapsto \mathbb{R}^2$, for a given $T_{\mathsf{f}} > 0$. Furthermore, $\mathbf{G}_i(\cdot), \mathbf{H}_i(\cdot) \in \mathcal{L}^\infty([0, T_{\mathsf{f}}], \mathbb{R}^{2\times 2})$, where $\mathcal{L}^\infty([0, T_{\mathsf{f}}], \mathbb{R}^{2\times 2})$ denotes the space of (almost everywhere) bounded functions $\mathbf{M} : [0, T_{\mathsf{f}}] \mapsto \mathbb{R}^{2\times 2}$. In addition, we assume that $\mathbf{H}_i(t)$ is non-singular for all $t \geq 0$ (that is, the system is *fully actuated* at all times). Finally, $f_i(\cdot) \in \mathcal{L}^2([0, T_{\mathsf{f}}], \mathbb{R}^2)$ is an externally applied reference signal.

[1] The *combinatorial complexity* of a generalized Voronoi diagram corresponds to the total number of the connected components of all the generalized cells that comprise the generalized Voronoi partition, the total number of "faces" or "curved edges" (generalizations of Voronoi edges) that enclose these sets and their corresponding vertices (generalizations of Voronoi vertices).

The objectives of the i-th vehicle are: 1) to reach a neighborhood of a desired terminal position $\mathsf{x}_\mathsf{f} \in \mathbb{R}^2$ at a fixed final time T_f with a small terminal speed, that is, a neighborhood of the point $\mathsf{z}_\mathsf{f} := [\mathsf{x}_\mathsf{f}^{\mathrm{T}},\ 0]^{\mathrm{T}} \in \mathcal{X}(0)$, and 2) to achieve this transition without incurring a significant cost (for example, the transition does not require an excessive amount of control effort).

Next, we formulate the steering problem in a coordinate system where the terminal state is always the origin. In particular, let $\mathsf{y}_i := \mathsf{z}_i - \mathsf{z}_\mathsf{f}$ and $\bar{\mathsf{y}}_i := \bar{\mathsf{z}}_i - \mathsf{z}_\mathsf{f}$. Then, Eq. (1) becomes

$$\dot{\mathsf{y}}_i = \mathbf{A}_i(t)\mathsf{y}_i + \mathbf{B}_i(t)u_i(t) + \mathsf{c}_i(t), \quad \mathsf{y}_i(0) = \bar{\mathsf{y}}_i, \qquad (2)$$

where

$$\mathbf{A}_i(t) := \begin{bmatrix} \mathbf{0} & \mathbf{I} \\ \mathbf{0} & \mathbf{G}_i(t) \end{bmatrix},\ \mathbf{B}_i(t) := \begin{bmatrix} \mathbf{0} \\ \mathbf{H}_i(t) \end{bmatrix},$$
$$\mathsf{c}_i(t) := [0,\ f_i^{\mathrm{T}}(t)]^{\mathrm{T}} \ \text{ (note that } \mathbf{A}_i(t)\mathsf{z}_\mathsf{f} \equiv 0).$$

Next we consider the following optimal control problem.

Problem 1 *Let $\mathbf{Q}_i = \mathbf{Q}_i^T > \mathbf{0}$ and $\varrho_i > 0$. Given a fixed final time $T_\mathsf{f} > 0$, find a control input $u_i^\circ \in \mathcal{L}^2([0, T_\mathsf{f}], \mathbb{R}^2)$ that minimizes the performance index*

$$\mathcal{J}_i(u_i, \bar{\mathsf{y}}_i) := \tfrac{1}{2}\,\mathsf{y}_i^T(T_\mathsf{f})\mathbf{Q}_i\mathsf{y}_i(T_\mathsf{f}) + \tfrac{1}{2\varrho_i}\int_0^{T_\mathsf{f}} |u_i(t)|^2 \mathrm{d}t, \quad (3)$$

subject to the dynamic constraint (2).

Remark 1 The weight $\varrho_i > 0$ is selected in accordance with the so-called Bryson and Ho rule [19, pp. 149] for linear quadratic optimization problems. The selection of the matrix $\mathbf{Q}_i$, which weighs the penalty placed on the terminal distance error $|\mathsf{y}_i(T_\mathsf{f})|$, can be done similarly. In particular, by increasing $\|\mathbf{Q}_i\|$, where $\|\cdot\|$ is any sub-multiplicative matrix norm, the terminal distance error decreases accordingly.

Before we address Problem 1, we shall briefly discuss when does a square integrable control law that transfers the i-th vehicle to any neighborhood of the target, regardless of how small the terminal distance error $|\mathsf{y}_i(T_\mathsf{f})|$ is required to be (by appropriately selecting, for example, the weighting matrix $\mathbf{Q}_i$), exist.

Assumption 1 *Let $T_\mathsf{f} > 0$ be given and let $\mathbf{\Phi}_i(0,t)$ denote the state transition matrix of the linear system $\dot{\xi}_i = \mathbf{A}_i(t)\xi_i$. Then, $\mathbf{W}_i(T_\mathsf{f}) = \mathbf{W}_i^T(T_\mathsf{f}) > \mathbf{0}$, for all $i \in \mathcal{I}_n$, where*

$$\mathbf{W}_i(t) := \int_0^t \mathbf{\Phi}_i(0,\sigma)\mathbf{B}_i(\sigma)\mathbf{B}_i^T(\sigma)\mathbf{\Phi}_i^T(0,\sigma)\mathrm{d}\sigma.$$

Under Assumption 1, the control law $u_i(\cdot) \in \mathcal{L}^2([0, T_\mathsf{f}], \mathbb{R}^2)$, where

$$u_i(t) = \mathbf{B}_i^{\mathrm{T}}(t)\mathbf{\Phi}_i^{\mathrm{T}}(0,t)\mathbf{W}_i^{-1}(T_\mathsf{f})(\mathbf{\Phi}_i(0,T_\mathsf{f})\mathsf{z}_\mathsf{f} - \bar{\mathsf{z}}_i) - \mathbf{H}_i^{-1}(t)f_i(t), \qquad (4)$$

will transfer the system (1) (respectively, the system (2)) from an arbitrary initial state $\bar{\mathsf{z}}_i$ (respectively, $\bar{\mathsf{y}}_i$) to any terminal state z_f (respectively, the origin) with zero terminal distance error at time $t = T_\mathsf{f}$ (see, for example, Corollary 2.3 and 2.5, and Eq. (2.23) in [21]).

Next we present the solution to Problem 1.

Proposition 1 *Let Assumption 1 hold and let $\varrho_i > 0, T_\mathsf{f} > 0$ be given. Then, for every $i \in \mathcal{I}_n$, there exists a unique triple $(\mathbf{S}_i(t), \mathsf{k}_i(t), m_i(t))$, where $\mathbf{S}_i(t) \in \mathbb{R}^{4\times 4}$ and $\mathbf{S}_i(t) = \mathbf{S}_i^T(t) \geq \mathbf{0}$, $\mathsf{k}_i(t) \in \mathbb{R}^4$, and $m_i(t) \in \mathbb{R}$, for all $t \in [0, T_\mathsf{f}]$, which satisfies the following set of equations*

$$\begin{aligned} -\dot{\mathbf{S}}_i &= \mathbf{S}_i\mathbf{A}_i(t) + \mathbf{A}_i^T(t)\mathbf{S}_i - {}^1\!/_{\varrho_i}\mathbf{S}_i\mathbf{B}_i(t)\mathbf{B}_i^T(t)\mathbf{S}_i, \\ -\dot{\mathsf{k}}_i &= \mathbf{A}_i^T(t)\mathsf{k}_i + \mathbf{S}\mathsf{c}_i(t) - {}^1\!/_{\varrho_i}\mathbf{S}_i\mathbf{B}_i(t)\mathbf{B}_i^T(t)\mathsf{k}_i, \\ -\dot{m}_i &= \mathsf{k}_i^T\mathsf{c}_i(t) - {}^1\!/_{2\varrho_i}\mathsf{k}_i\mathbf{B}_i(t)\mathbf{B}_i^T(t)\mathsf{k}_i, \end{aligned} \qquad (5)$$

with boundary conditions

$$\mathbf{S}_i(T_\mathsf{f}) = \mathbf{Q}_i, \quad \mathsf{k}_i(T_\mathsf{f}) = 0, \quad m_i(T_\mathsf{f}) = 0, \qquad (6)$$

such that the optimal control law that solves Problem 1 is given by

$$u_i^\circ(t, \mathsf{y}_i^\circ) = -{}^1\!/_{\varrho_i}\,\mathbf{B}_i^T(t)[\mathbf{S}_i(t)\mathsf{y}_i^\circ + \mathsf{k}_i(t)]. \qquad (7)$$

In addition, the corresponding minimum cost $\mathcal{J}_i^\circ(\bar{\mathsf{y}}_i) := \mathcal{J}_i(u_i^\circ, \bar{\mathsf{y}}_i)$ (value function of Problem 1) is given by

$$\mathcal{J}_i^\circ(\bar{\mathsf{y}}_i) = {}^1\!/_2\,\bar{\mathsf{y}}_i^T\mathbf{S}_i(0)\bar{\mathsf{y}}_i + \mathsf{k}_i^T(0)\bar{\mathsf{y}}_i + m_i(0). \qquad (8)$$

PROOF. The reader may refer to [22, pp. 228-229].

Remark 2 Note that for a given $T_\mathsf{f} > 0$ and $i \in \mathcal{I}_n$, the triple $(\mathbf{S}_i(t), \mathsf{k}_i(t), m_i(t))$ is independent of the terminal state z_f, for all $t \in [0, T_\mathsf{f}]$. In addition, if the matrices and the parameters that appear in Eqs. (2) and (3) are not the same for all $i \in \mathcal{I}_n$, then the triple $(\mathbf{S}_i(t), \mathsf{k}_i(t), m_i(t))$ may not be the same for all $i \in \mathcal{I}_n$ as well.

An important observation is that the value function $\mathcal{J}_i^\circ(\bar{\mathsf{y}}_i)$ of Problem 1 is not necessarily minimized at $\bar{\mathsf{y}}_i = 0$ (that is, when the initial and terminal positions are the same).

Proposition 2 *Let Assumption 1 hold and let $T_\mathsf{f} > 0$ be given. Then the value function $\mathcal{J}_i^\circ(\bar{\mathsf{y}}_i)$ of Problem 1 is nonnegative and finite for all $\bar{\mathsf{y}}_i \in \mathbb{R}^4$. If, in addition, $\mathbf{S}_i(0) = \mathbf{S}_i^T(0) > \mathbf{0}$, then $\mathcal{J}_i^\circ(\bar{\mathsf{y}}_i)$ is minimized at $\bar{\mathsf{y}}_i^\circ = -\mathbf{S}_i^{-1}(0)\mathsf{k}_i(0)$, where*

$$\mathcal{J}_i^\circ(\bar{\mathsf{y}}_i^\circ) = -{}^1\!/_2\,\mathsf{k}_i^T(0)\mathbf{S}_i^{-1}(0)\mathsf{k}_i(0) + m_i(0). \qquad (9)$$

PROOF. The cost $\mathcal{J}_i^\circ(\bar{\mathsf{y}}_i)$ is a convex function given that its Hessian matrix, denoted by $\mathcal{H}(\mathcal{J}_i^\circ(\bar{\mathsf{y}}_i))$, satisfies $\mathcal{H}(\mathcal{J}_i^\circ(\bar{\mathsf{y}}_i)) = \mathbf{S}_i(0) > \mathbf{0}$. Therefore, the cost $\mathcal{J}_i^\circ$ attains its minimum at $\bar{\mathsf{y}}_i = \bar{\mathsf{y}}_i^\circ$, where $\bar{\mathsf{y}}_i^\circ$ is the unique solution of the equation $\nabla\mathcal{J}_i^\circ(\bar{\mathsf{y}}_i) = 0$. The rest of the proof is straightforward and is omitted.

3 Formulation of the Partitioning Problem

In this section, we will formulate a generalized Voronoi partitioning problem, where the value function of Problem 1 will serve as the proximity metric that will determine the proximity relations between the vehicles and arbitrary target points. The partition space consists of all the possible terminal states $\mathsf{z} = [\mathsf{x}^{\mathrm{T}},\ 0]^{\mathrm{T}} \in \mathcal{X}(0)$. Note that the partition space is a space of positions (the terminal velocities are fixed to zero), and consequently, the proximity metric should be a function of the position vector of each vehicle only, whereas the initial velocities, which are non-zero in general, should serve as constant parameters. In particular, we take the proximity metric to be the restriction of the value function of Problem 1 given in Eq. (8) to the position space $\mathcal{X}(0)$. We denote this function by $\mathsf{x} \mapsto c_i(\mathsf{x}; \bar{\mathsf{z}}_i)$, where

$$c_i(\mathsf{x}; \bar{\mathsf{z}}_i) := \mathcal{J}_i^\circ(\bar{\mathsf{z}}_i - \mathsf{z}(\mathsf{x})),\ \mathsf{z}(\mathsf{x}) := [\mathsf{x}^{\mathrm{T}},\ 0]^{\mathrm{T}} \in \mathcal{X}(0), \quad (10)$$

for $i \in \mathcal{I}_n$. Note that the cost $c_i(\mathsf{x}; \bar{\mathsf{z}}_i)$ is the minimum control effort required to drive the system (1) from the prescribed initial state $\bar{\mathsf{z}}_i$ to a neighborhood of the point $\mathsf{z} := [\mathsf{x}^{\mathrm{T}},\ 0]^{\mathrm{T}} \in \mathcal{X}(0)$ at a given time T_{f} (transition cost function).

Next, we formulate the generalized Voronoi partitioning problem.

Problem 2 *Let $\overline{\mathcal{Z}} := \{\bar{\mathsf{z}}_i \in \mathbb{R}^4 :\ i \in \mathcal{I}_n\}$ be given. Then, determine a partition $\mathfrak{V} = \{\mathfrak{V}_i :\ i \in \mathcal{I}_n\}$ of $\mathcal{X}(0)$ such that*

(1) $\mathcal{X}(0) = \bigcup_{i\in\mathcal{I}_n} \mathfrak{V}_i$,
(2) $\operatorname{int}\mathfrak{V}_i \cap \operatorname{int}\mathfrak{V}_j = \varnothing$, for all $i, j \in \mathcal{I}_n$, $i \neq j$,
(3) A point $\mathsf{z} = [\mathsf{x}^T,\ 0]^T \in \mathcal{X}(0)$ belongs to $\mathfrak{V}_i$ if, and only if, $c_i(\mathsf{x}; \bar{\mathsf{z}}_i) \leq c_j(\mathsf{x}; \bar{\mathsf{z}}_j)$, for all $j \in \mathcal{I}_n$, where $c_\ell(\mathsf{x}; \bar{\mathsf{z}}_\ell)$, $\ell \in \{i, j\}$, is given by Eq. (10).

Remark 3 Note that the partition $\mathfrak{V}$ that solves Problem 2 is a generalized Voronoi diagram with respect to an anisotropic state-dependent (pseudo-) metric.

4 The Solution to the Partitioning Problem

In this Section, we show that the solution to the Problem 2 can be associated with two classes of generalized Voronoi diagrams, namely power and affine Voronoi diagrams, for the computation of which efficient techniques exist in the literature.

4.1 Structure of the Proximity Metric Induced by the Minimum Control Effort

Next, we show that the proximity metric of Problem 2 can be expressed as a particular non-homogeneous quadratic form.

Proposition 3 *Let $\bar{\mathsf{z}}_i = [\bar{\mathsf{x}}_i^T,\ \bar{\mathsf{v}}_i^T]^T \in \overline{\mathcal{Z}}$ and let us assume that $\mathbf{S}_i(0) = \mathbf{S}_i^T(0) > \mathbf{0}$. Then, there exists a matrix $\mathbf{\Gamma}_i \in \mathbb{R}^{2\times 2}$, where $\mathbf{\Gamma}_i = \mathbf{\Gamma}_i^T > \mathbf{0}$, a vector $\bar{\mathsf{x}}_i^\star = \bar{\mathsf{x}}_i^\star(\bar{\mathsf{z}}_i) \in \mathbb{R}^2$, and a scalar $\mu_i^\star = \mu_i^\star(\bar{\mathsf{v}}_i)$ such that Eq.* (10) *can be written as follows*

$$c_i(\mathsf{x}; \bar{\mathsf{z}}_i) = (\mathsf{x} - \bar{\mathsf{x}}_i^\star(\bar{\mathsf{z}}_i))^T \mathbf{\Gamma}_i (\mathsf{x} - \bar{\mathsf{x}}_i^\star(\bar{\mathsf{z}}_i)) + \mu_i^\star(\bar{\mathsf{v}}_i), \quad (11)$$

for $i \in \mathcal{I}_n$.

PROOF. The cost given in Eq. (8) can be written as a non-homogenous quadratic form as follows

$$\mathcal{Q}(\delta\mathsf{z}; \mathbf{\Sigma}) = \delta\mathsf{z}^{\mathrm{T}} \mathbf{\Sigma} \delta\mathsf{z} + \kappa^{\mathrm{T}} \delta\mathsf{z} + \mu, \quad (12)$$

where $\delta\mathsf{z} := \bar{\mathsf{z}}_i - \mathsf{z}$, $\mathbf{\Sigma} := {}^1\!/_2\, \mathbf{S}_i(0)$, $\kappa := \mathsf{k}_i(0)$, and $\mu = m_i(0)$. Next we consider the following decompositions of the matrix $\mathbf{\Sigma}$ and the vectors κ, $\delta\mathsf{z}$,

$$\mathbf{\Sigma} = \begin{bmatrix} \mathbf{\Sigma}_{11} & \mathbf{\Sigma}_{12} \\ \mathbf{\Sigma}_{21} & \mathbf{\Sigma}_{22} \end{bmatrix}, \qquad \kappa = \begin{bmatrix} \kappa_1 \\ \kappa_2 \end{bmatrix}, \qquad \delta\mathsf{z} = \begin{bmatrix} \delta\mathsf{x} \\ \bar{\mathsf{v}}_i \end{bmatrix},$$

where $\delta\mathsf{x} := \bar{\mathsf{x}}_i - \mathsf{x}$, $\kappa_1, \kappa_2 \in \mathbb{R}^2$ and $\mathbf{\Sigma}_{ij} \in \mathbb{R}^{2\times 2}$, where $i, j \in \{1, 2\}$. After some algebraic manipulation, it follows that Eq. (12) can be written as follows

$$\begin{aligned} \mathcal{Q}(\delta\mathsf{x}; \bar{\mathsf{v}}_i, \mathbf{\Sigma}) &= \delta\mathsf{x}^{\mathrm{T}} \mathbf{\Sigma}_{11} \delta\mathsf{x} + \bar{\mathsf{v}}_i^{\mathrm{T}} (\mathbf{\Sigma}_{21} + \mathbf{\Sigma}_{12}^{\mathrm{T}}) \delta\mathsf{x} \\ &\quad + \bar{\mathsf{v}}_i^{\mathrm{T}} \mathbf{\Sigma}_{22} \bar{\mathsf{v}}_i + \kappa_1^{\mathrm{T}} \delta\mathsf{x} + \kappa_2 \bar{\mathsf{v}}_i + \mu \\ &= \delta\mathsf{x}^{\mathrm{T}} \mathbf{\Sigma}_{11} \delta\mathsf{x} + \mathsf{g}^{\mathrm{T}}(\bar{\mathsf{v}}_i) \delta\mathsf{x} + \mathcal{D}(\bar{\mathsf{v}}_i, \mathbf{\Sigma}), \end{aligned} \quad (13)$$

where $\mathcal{D}(\bar{\mathsf{v}}_i, \mathbf{\Sigma}) := \bar{\mathsf{v}}_i^{\mathrm{T}} \mathbf{\Sigma}_{22} \bar{\mathsf{v}}_i + \kappa_2^{\mathrm{T}} \bar{\mathsf{v}}_i + \mu$, and $\mathsf{g}(\bar{\mathsf{v}}_i) := (\mathbf{\Sigma}_{21}^{\mathrm{T}} + \mathbf{\Sigma}_{12}) \bar{\mathsf{v}}_i + \kappa_1$. Next, we consider the transformation $\mathsf{p} = \mathbf{\Sigma}_{11}^{1/2} \delta\mathsf{x}$, where $\mathbf{\Sigma}_{11}^{1/2} = (\mathbf{\Sigma}_{11}^{1/2})^{\mathrm{T}} > \mathbf{0}$ denotes the square root of the matrix $\mathbf{\Sigma}_{11}$ [2]. Then Eq. (12) reduces to

$$\mathcal{Q}(\mathsf{p}; \bar{\mathsf{v}}_i) = \mathsf{p}^{\mathrm{T}} \mathsf{p} + \mathsf{g}^{\mathrm{T}}(\bar{\mathsf{v}}_i) \mathbf{\Sigma}_{11}^{-1/2} \mathsf{p} + \mathcal{D}(\bar{\mathsf{v}}_i), \quad (14)$$

which, after some algebraic manipulation, gives

$$\begin{aligned} \mathcal{Q}(\mathsf{p}; \bar{\mathsf{v}}_i) &= (\mathsf{p} + {}^1\!/_2\, \mathbf{\Sigma}_{11}^{-1/2} \mathsf{g}(\bar{\mathsf{v}}_i))^{\mathrm{T}} (\mathsf{p} + {}^1\!/_2 \mathbf{\Sigma}_{11}^{-1/2} \mathsf{g}(\bar{\mathsf{v}}_i)) \\ &\quad + \mathcal{D}(\bar{\mathsf{v}}_i) - {}^1\!/_4\, \mathsf{g}^{\mathrm{T}}(\bar{\mathsf{v}}_i) \mathbf{\Sigma}_{11}^{-1} \mathsf{g}(\bar{\mathsf{v}}_i), \\ &= (\mathsf{p} + \mathsf{p}^\star(\bar{\mathsf{v}}_i))^{\mathrm{T}} (\mathsf{p} + \mathsf{p}^\star(\bar{\mathsf{v}}_i)) + \mu_i^\star(\bar{\mathsf{v}}_i), \end{aligned} \quad (15)$$

[2] It is easy to show that when $\mathbf{\Sigma} = \mathbf{\Sigma}^{\mathrm{T}} > \mathbf{0}$, then $\mathbf{\Sigma}_{11} = \mathbf{\Sigma}_{11}^{\mathrm{T}} > \mathbf{0}$ and consequently, $\mathbf{\Sigma}_{11}^{1/2} = (\mathbf{\Sigma}_{11}^{1/2})^{\mathrm{T}} > \mathbf{0}$.

where $\mathsf{p}^\star(\bar{\mathsf{v}}_i) := {}^1\!/_2\,\boldsymbol{\Sigma}_{11}^{-1/2}\mathsf{g}(\bar{\mathsf{v}}_i)$ and $\mu_i^\star(\bar{\mathsf{v}}_i) := \mathcal{D}(\bar{\mathsf{v}}_i) - {}^1\!/_4\,\mathsf{g}^{\mathrm{T}}(\bar{\mathsf{v}}_i)\boldsymbol{\Sigma}_{11}^{-1}\mathsf{g}(\bar{\mathsf{v}}_i)$. Therefore, Eq. (10), can be written as follows

$$c_i(\mathsf{x};\bar{\mathsf{z}}_i) = (\mathsf{x} - \bar{\mathsf{x}}_i^\star(\bar{\mathsf{z}}_i))^{\mathrm{T}}\boldsymbol{\Sigma}_{11}(\mathsf{x} - \bar{\mathsf{x}}_i^\star(\bar{\mathsf{z}}_i)) + \mu_i^\star(\bar{\mathsf{v}}_i),$$

where $\bar{\mathsf{x}}_i^\star(\bar{\mathsf{z}}_i) = \bar{\mathsf{x}}_i + \boldsymbol{\Sigma}_{11}^{-1/2}\mathsf{p}^\star(\bar{\mathsf{v}}_i)$, and the result follows readily.

Remark 4 Note that the matrix $\boldsymbol{\Gamma}_i$ is independent of the terminal state z given that the triple $(\mathbf{S}_i, \mathsf{k}_i, m_i)$ is also independent of z (or equivalently, the initial state $\bar{\mathsf{y}}_i$). It does depends, however, on the index of the vehicle, and in particular, the matrices that appear in Eqs. (2) and (3).

Corollary 1 *Let $\bar{\mathsf{z}}_i \in \overline{\mathcal{Z}}$ and let us assume that $\mathbf{S}_i(0) = \mathbf{S}_i^T(0) > \mathbf{0}$. Then the cost function $\mathsf{x} \mapsto c_i(\mathsf{x};\bar{\mathsf{z}}_i)$ defined in Eq. (10) attains its minimum value at $\mathsf{x}_i^\circ = \bar{\mathsf{x}}_i^\star(\bar{\mathsf{z}}_i)$ and, in addition, $c_i(\mathsf{x}_i^\circ;\bar{\mathsf{z}}_i) = \mu_i^\star(\bar{\mathsf{v}}_i) = \min_{\mathsf{x}\in\mathbb{R}^2} c_i(\mathsf{x};\bar{\mathsf{z}}_i)$.*

4.2 Characterization of the Solution to the Partitioning Problem

Next, we address Problem 2 by exploiting the particular structure of its proximity metric. To this aim, we shall examine both the cases when 1) the quantities $\boldsymbol{\Gamma}_i$, $\bar{\mathsf{x}}_i^\star(\cdot)$ and $\mu_i^\star(\cdot)$ are not necessarily the same for all $i \in \mathcal{I}_n$ (in this case, the vehicles may not have identical transition cost functions c_i), and 2) $\boldsymbol{\Gamma}_i = \boldsymbol{\Gamma}_j$, $\bar{\mathsf{x}}_i^\star(\cdot) = \bar{\mathsf{x}}_j^\star(\cdot)$ and $\mu_i^\star(\cdot) = \mu_j^\star(\cdot)$, for all $i, j \in \mathcal{I}_n$ (the vehicles now have identical transition cost functions c_i).

4.2.1 The General Case When the Transition Cost Function is not Necessarily the Same for All Vehicles

We consider the case when the quantities $\boldsymbol{\Gamma}_i$, $\bar{\mathsf{x}}_i^\star(\cdot)$ and $\mu_i^\star(\cdot)$ are not necessarily the same for all $i \in \mathcal{I}_n$. In this case, the bisector $\mathcal{B}_{ij}$ that corresponds to the generators $\bar{\mathsf{z}}_i$ and $\bar{\mathsf{z}}_j \in \overline{\mathcal{Z}}$, that is, the loci of all points $\mathsf{z} = [\mathsf{x}^{\mathrm{T}},\ 0]^{\mathrm{T}} \in \mathcal{X}(0)$ for which $c_i(\mathsf{x};\bar{\mathsf{z}}_i) = c_j(\mathsf{x};\bar{\mathsf{z}}_j)$, is determined by the following equation

$$\mathsf{x}^{\mathrm{T}}(\boldsymbol{\Gamma}_i - \boldsymbol{\Gamma}_j)\mathsf{x} + 2(\boldsymbol{\Gamma}_j\bar{\mathsf{x}}_j^\star - \boldsymbol{\Gamma}_i\bar{\mathsf{x}}_i^\star)^{\mathrm{T}}\mathsf{x} + \pi_i^2 - \pi_j^2 = 0, \quad (16)$$

where $\bar{\mathsf{x}}_\ell^\star := \bar{\mathsf{x}}_\ell^\star(\bar{\mathsf{z}}_\ell)$ and $\pi_\ell^2 := \mu_\ell^\star(\bar{\mathsf{v}}_\ell) + (\bar{\mathsf{x}}_\ell^\star)^{\mathrm{T}}\boldsymbol{\Gamma}_\ell\,\bar{\mathsf{x}}_\ell^\star$, $\ell \in \{i, j\}$. We immediately conclude that $\mathcal{B}_{ij}$ is a conic section. Next we state the main result of this section.

Theorem 1 *Let $\mathfrak{V} := \{\mathfrak{V}_i,\ i \in \mathcal{I}_n\}$ denote the partition that solves Problem 2 and let $\mathfrak{V}^\star := \{\mathfrak{V}_i^\star,\ i \in \mathcal{I}_n\}$ denote the power Voronoi diagram generated by the set of spheres $\overline{\mathcal{S}} := \{\mathcal{S}_i,\ i \in \mathcal{I}_n\}$ in $\mathbb{R}^5$, where the sphere $\mathcal{S}_i$ is centered at the point σ_i with coordinates*

$$\sigma_i := \left[(\boldsymbol{\Gamma}_i\bar{\mathsf{x}}_i^\star)^T, -\tfrac{1}{2}\boldsymbol{\Gamma}_i^{[1,1]}, -\boldsymbol{\Gamma}_i^{[1,2]}, -\tfrac{1}{2}\boldsymbol{\Gamma}_i^{[2,2]}\right]^T, \quad (17)$$

where $\boldsymbol{\Gamma}_i^{[k,\ell]}$ denotes the (k,ℓ) element of the matrix $\boldsymbol{\Gamma}_i$, and the power distance of the origin[3] *with respect to $\mathcal{S}_i$ is equal to $\pi_i^2 := \mu_i^\star(\bar{\mathsf{v}}_i) + (\bar{\mathsf{x}}_i^\star)^T\boldsymbol{\Gamma}_i\,\bar{\mathsf{x}}_i^\star$. Then a point $\mathsf{z} = [\mathsf{x}^T,\ 0]^T$, where $\mathsf{x} = [x,\ y]^T$, belongs to $\mathfrak{V}_i$ if, and only if, the point $\mathsf{r} = \mathsf{r}(\mathsf{z}) \in \mathbb{R}^5$, where $\mathsf{r}(\mathsf{z}) := [x,\ y,\ x^2,\ xy,\ y^2]^T$, belongs to the cell $\mathfrak{V}_i^\star$. Finally, $\mathfrak{V}^\star$ has combinatorial complexity $\Theta(n^3)$ and can be computed in time $\mathcal{O}(n\log n + n^3)$.*

PROOF. A point $\mathsf{z} = [\mathsf{x}^{\mathrm{T}},\ 0]^{\mathrm{T}} \in \mathcal{X}(0)$ belongs to $\mathfrak{V}_i$ if, and only if, $c_i(\mathsf{x};\bar{\mathsf{z}}_i) \le c_j(\mathsf{x};\bar{\mathsf{z}}_i)$, for all $j \in \mathcal{I}_n$, or equivalently,

$$\mathsf{x}^{\mathrm{T}}\boldsymbol{\Gamma}_i\mathsf{x} - 2\mathsf{x}^{\mathrm{T}}\boldsymbol{\Gamma}_i\bar{\mathsf{x}}_i^\star + \pi_i^2 \le \mathsf{x}^{\mathrm{T}}\boldsymbol{\Gamma}_j\mathsf{x} - 2\mathsf{x}^{\mathrm{T}}\boldsymbol{\Gamma}_j\bar{\mathsf{x}}_j^\star + \pi_j^2, \quad (18)$$

where $\bar{\mathsf{x}}_\ell^\star := \bar{\mathsf{x}}_\ell^\star(\bar{\mathsf{z}}_\ell)$ and $\pi_\ell^2 := \mu_\ell^\star + (\bar{\mathsf{x}}_\ell^\star)^{\mathrm{T}}\boldsymbol{\Gamma}_\ell\,\bar{\mathsf{x}}_\ell^\star$, for $\ell \in \{i, j\}$. Now let $\mathsf{r}(\mathsf{z}) := [x,\ y,\ x^2,\ xy,\ y^2]^{\mathrm{T}} \in \mathbb{R}^5$. Then, it is easy to verify (see [23]) that Eq. (18) can be written as follows

$$|\mathsf{r} - \sigma_i|^2 - (|\sigma_i|^2 - \pi_i^2) \le |\mathsf{r} - \sigma_j|^2 - (|\sigma_j|^2 - \pi_j^2), \quad (19)$$

where $\sigma_i \in \mathbb{R}^5$ is given by (17). Therefore, the point z belongs to the cell $\mathfrak{V}_i$ associated with the point $\bar{\mathsf{z}}_i \in \overline{\mathcal{Z}}$ if, and only if, the power distance of the point $\mathsf{r}(\mathsf{z})$ with respect to the sphere $\mathcal{S}_i$ is no greater than its power distance with respect to any other sphere from $\overline{\mathcal{S}}$. Equivalently, $\mathsf{z} \in \mathfrak{V}_i$ if, and only if, $\mathsf{r} \in \mathfrak{V}_i^\star$.

The result on the combinatorial complexity of $\mathfrak{V}^\star$ and the computational time follow immediately from Corollary 18.1.2 [4, p. 435]. ■

Remark 5 The notation $\Theta(\cdot)$ has the following meaning: Given a function $f : \mathbb{N} \mapsto [0,\infty)$, then $\Theta(f(n))$ denotes the set of functions $g : \mathbb{N} \mapsto [0,\infty)$ that satisfy $c_1 f(n) \le g(n) \le c_2 f(n)$, for all $n \ge n_0$, where $c_1, c_2 > 0$ and $n_0 \in \mathbb{N}$.

Remark 6 Proposition 1 implies that the solution to Problem 2 for the general case, when the quantities $\boldsymbol{\Gamma}_i$, $\bar{\mathsf{x}}_i^\star(\cdot)$, and $\mu_i^\star(\cdot)$ are not necessarily identical for all $i \in \mathcal{I}_n$, reduces to the construction of a power Voronoi diagram generated by a set of spheres in $\mathbb{R}^5$; the restriction of this power Voronoi diagram to the two-dimensional partition space $\mathcal{X}(0)$ will furnish the solution to the partitioning problem. Practically, this means that one can address the partitioning problem proposed in this work by employing well known algorithms from the literature of computational geometry (see, for example, [3]).

4.2.2 The Case When the Value Function is the Same for All Vehicles

Next, we consider the case when $\boldsymbol{\Gamma}_i = \boldsymbol{\Gamma}_j$, $\bar{\mathsf{x}}_i^\star(\cdot) = \bar{\mathsf{x}}_j^\star(\cdot)$ and $\mu_i^\star(\cdot) = \mu_j^\star(\cdot)$, for all $i, j \in \mathcal{I}_n$, in which case we sim-

[3] The power distance of a point x with respect to a sphere $\mathcal{S}$ is the square of the length of the line segment emanating from x that is tangent to $\mathcal{S}$ and terminating at the point of tangency.

ply write, respectively, $\mathbf{\Gamma}, \bar{\mathsf{x}}^\star(\cdot)$ and $\mu^\star(\cdot)$. The proximity metric of Problem 2 becomes

$$c(\mathsf{x}, \bar{\mathsf{z}}_i) := (\mathsf{x} - \bar{\mathsf{x}}^\star(\bar{\mathsf{z}}_i))^{\mathrm{T}} \mathbf{\Gamma} (\mathsf{x} - \bar{\mathsf{x}}^\star(\bar{\mathsf{z}}_i)) + \mu^\star(\bar{\mathsf{v}}_i). \quad (20)$$

Next we associate the solution to Problem 2 with an affine Voronoi diagram [4] in $\mathbb{R}^2$.

Proposition 4 *Let $\mathfrak{V} := \{\mathfrak{V}_i,\ i \in \mathcal{I}_n\}$ denote the generalized Voronoi diagram that solves Problem 2 for a given set of generators $\overline{\mathcal{Z}}$, when the proximity metric is given by Eq. (20). Then, a point $\mathsf{z} = [\mathsf{x}^T,\ 0]^T$, where $\mathsf{x} = [x,\ y]^T$, belongs to $\mathfrak{V}_i$ if, and only if, $\mathsf{x} \in \mathfrak{V}_i^\star$, where $\mathfrak{V}^\star := \{\mathfrak{V}_i^\star,\ i \in \mathcal{I}_n\}$ denote the generalized Voronoi diagram generated by the point-set $\overline{\mathcal{X}}^\star := \{\bar{\mathsf{x}}_i^\star = \bar{\mathsf{x}}^\star(\bar{\mathsf{z}}_i),\ i \in \mathcal{I}_n\}$ with respect to the proximity metric $c^\star : \mathbb{R}^2 \mapsto [0, \infty)$, where*

$$c^\star(\mathsf{x}; \bar{\mathsf{z}}_i^\star) := (\mathsf{x} - \bar{\mathsf{x}}_i^\star)^T \mathbf{\Gamma} (\mathsf{x} - \bar{\mathsf{x}}_i^\star) + \mu^\star(\bar{\mathsf{v}}_i),\ \bar{\mathsf{z}}_i^\star := [(\bar{\mathsf{x}}_i^\star)^T,\ \bar{\mathsf{v}}_i^T]^T,$$

which is an affine Voronoi diagram in $\mathbb{R}^2$.

PROOF. Note that a point $\mathsf{z} = [\mathsf{x}^{\mathrm{T}},\ 0]^{\mathrm{T}}$ belongs to the cell $\mathfrak{V}_i \in \mathfrak{V}$ associated with the generator $\bar{\mathsf{z}}_i \in \overline{\mathcal{Z}}$ if, and only if, $c(\mathsf{x}; \bar{\mathsf{z}}_i) \leq c(\mathsf{x}; \bar{\mathsf{z}}_j)$, for all $i \neq j$, or equivalently, $c^\star(\mathsf{x}; \bar{\mathsf{z}}_i^\star) \leq c^\star(\mathsf{x}; \bar{\mathsf{z}}_j^\star)$. Consequently, $\mathsf{z} \in \mathfrak{V}_i$ if, and only if, x belongs to the cell $\mathfrak{V}_i^\star \in \mathfrak{V}^\star$ associated with the generator $\bar{\mathsf{x}}_i^\star \in \overline{\mathcal{X}}^\star$.

To prove that $\mathfrak{V}^\star$ is an affine Voronoi diagram in $\mathbb{R}^2$, it suffices to show that the bisector $\mathcal{B}_{ij}^\star$ that corresponds to $\bar{\mathsf{x}}_i^\star$ and $\bar{\mathsf{x}}_j^\star \in \overline{\mathcal{X}}^\star$, where $i \neq j$, is a straight line. In particular, a point $\mathsf{x} \in \mathcal{B}_{ij}^\star$ if, and only if, $c^\star(\mathsf{x}; \bar{\mathsf{z}}_i^\star) = c^\star(\mathsf{x}; \bar{\mathsf{z}}_j^\star)$, which implies that

$$2(\bar{\mathsf{x}}_j^\star - \bar{\mathsf{x}}_i^\star)^{\mathrm{T}} \mathbf{\Gamma} \mathsf{x} + \pi_i^2 - \pi_j^2 = 0, \quad (21)$$

where $\pi_\ell^2 := \mu^\star(\bar{\mathsf{v}}_\ell) + (\bar{\mathsf{x}}_\ell^\star)^{\mathrm{T}} \mathbf{\Gamma} \bar{\mathsf{x}}_\ell^\star$, $\ell \in \{i, j\}$. Note that Eq. (21) describes a straight line in $\mathbb{R}^2$. This completes the proof. ■

Next we establish a direct correspondence between the solution to Problem 2 and a power Voronoi diagram generated by a set of circles.

Theorem 2 *Let $\mathfrak{V} := \{\mathfrak{V}_i,\ i \in \mathcal{I}_n\}$ be the generalized Voronoi diagram that solves Problem 2 and let $\mathfrak{V}^\star := \{\mathfrak{V}_i^\star,\ i \in \mathcal{I}_n\}$ denote the corresponding affine diagram generated by $\overline{\mathcal{X}}^\star$, which was introduced in Proposition 4. Then, $\mathfrak{V}^\star$ is the power Voronoi diagram generated by the set of circles $\overline{\mathcal{C}} := \{\mathcal{C}_i,\ i \in \mathcal{I}_n\}$, where the circle $\mathcal{C}_i$ is centered at the point $\mathbf{\Gamma} \bar{\mathsf{x}}_i^\star$ and the power distance of the origin with respect to $\mathcal{C}_i$ is equal to $\pi_i^2 := \mu^\star(\bar{\mathsf{v}}_i) + (\bar{\mathsf{x}}_i^\star)^T \mathbf{\Gamma} \bar{\mathsf{x}}_i^\star$. In addition, $\mathfrak{V}^\star$ has combinatorial complexity $\Theta(n)$ and can be computed in time $\Theta(n \log n + n)$.*

PROOF. The proof that $\mathfrak{V}^\star := \{\mathfrak{V}_i^\star,\ i \in \mathcal{I}_n\}$ is a power Voronoi diagram in $\mathbb{R}^2$ is a direct application of Theorem 18.2.2 from [4, p. 438], whereas the result on the combinatorial complexity of $\mathfrak{V}^\star$ and the computational time follow immediately from Theorem 18.2.3 from [4, p. 439].

Remark 7 Theorem 2 implies that Problem 2 can be reduced to the problem of computing an affine diagram, which is, in turn, associated with a power Voronoi diagram generated by a set of circles for the computation of which efficient algorithms exist in the literature [3]. In addition, the bounds on the combinatorial complexity and the computational time reveal that the affine diagram that solves Problem 2 is neither significantly more complex nor more expensive to compute than a standard Voronoi diagram generated by a point-set of n generators.

5 Simulation Results

In this section, we present simulation results that illustrate the previously presented theoretical developments. In particular, we consider a scenario with $n = 10$ vehicles, where the motion of the i-th vehicle is described by the following set of equations

$$\dot{\mathsf{x}}_i = \mathsf{v}_i,\ \ \dot{\mathsf{v}}_i = u_i(t), \quad \mathsf{x}_i(0) = \bar{\mathsf{x}}_i,\ \ \mathsf{v}_i(0) = \bar{\mathsf{v}}_i, \quad (22)$$

for which Assumption 1 is easily verified.

For the simulation purposes, we have used the following data: $\mathbf{Q} = \left[\begin{smallmatrix} \mathbf{Q}_d & \mathbf{I} \\ \mathbf{I} & \mathbf{Q}_d \end{smallmatrix}\right]$, $\mathbf{Q}_d = \left[\begin{smallmatrix} 2 & 1 \\ 1 & 2 \end{smallmatrix}\right]$, $T_{\mathsf{f}} = 2$. Figure 1 illustrates the generalized Voronoi diagram $\mathfrak{V}$, which solves Problem 2. For the computation of the diagrams, we have employed a partitioning algorithm, which is suitable for a large class of generalized Voronoi partitions and is based on the characterization of the lower envelope cost function $\underline{c} : \mathbb{R}^2 \mapsto [0, \infty)$, which is defined by $\underline{c}(\mathsf{x}) := \min_{\bar{\mathsf{z}}_i \in \overline{\mathcal{Z}}} c(\mathsf{x}; \bar{\mathsf{z}}_i)$ when the transiton cost function is the same for all the vehicles, and $\underline{c}(\mathsf{x}) := \min_{i \in \mathcal{I}_n} c_i(\mathsf{x}; \bar{\mathsf{z}}_i)$ otherwise (for more details on the implementation of this algorithm, the reader may refer to [16] and references therein). One may alternatively employ a more specialized algorithm for the computation of power diagrams, such as the (MAXIMAL) POWER DIAGRAM algorithm, which can be found in [24].

We consider both the case when ϱ_i is the same for all $i \in \mathcal{I}_n$, which implies, in turn, that $\mathbf{\Gamma}_i = \mathbf{\Gamma}_j, \bar{\mathsf{x}}_i^\star(\cdot) = \bar{\mathsf{x}}_j^\star(\cdot)$ and $\mu_i^\star(\cdot) = \mu_j^\star(\cdot)$, for all $i, j \in \mathcal{I}_n$ (Fig. 1(a)), or ϱ_i is not the same for all the vehicles, in which case $\mathbf{\Gamma}_i$, $\bar{\mathsf{x}}_i^\star(\cdot)$ and $\mu_i^\star(\cdot)$ are not the same for all $i \in \mathcal{I}_n$ (Fig. 1(b)). In particular, we take $\varrho_i = 2$ and $\varrho_i = i/5$ for the first and the second case, respectively. Each arrow in Fig. 1 cor-

[4] Affine Voronoi diagrams generated by a finite point set constitute a class of generalized Voronoi diagrams whose bisectors correspond to hyperplanes.

responds to the initial velocity vector $\bar{\mathrm{v}}_i \in \overline{\mathcal{V}}$ of the i-th vehicle, which is initially located at $\bar{\mathrm{x}}_i \in \overline{\mathcal{X}}$ (the locations of the generators are denoted by black crosses), whereas the dashed lines correspond to the standard Voronoi diagram generated by the point-set $\overline{\mathcal{X}}$. When $\varrho_i = 2$, for all $i \in \mathcal{I}_n$, then all the bisectors are straight lines, as illustrated in Fig. 1(a). By contrast, when $\varrho_i = i/5$, then some of the bisectors correspond to segments of conic sections, as illustrated in Fig. 1(b). The previous observations are in total agreement with the discussion in Section 4. In addition, we observe that all the cells that comprise the partition $\mathfrak{V}$ are convex in the first case but not all of them are convex in the second case (for example, the cell $\mathfrak{V}_6$ in Fig. 1(b) is non-convex).

Furthermore, we observe that both the generalized Voronoi diagrams illustrated in Fig. 1 are significantly different from the corresponding standard Voronoi diagram generated by the point-set $\overline{\mathcal{X}}$. We observe, for example, that the neighboring relations among the generators induced by the two different types of partitions differ significantly. Another important observation is that the generators of $\mathfrak{V}$ are not necessarily interior points of their corresponding cells in contrast with the standard Voronoi diagram.

Finally, Fig. 2 illustrates the level sets of the lower envelope cost function for the affine and the power Voronoi diagram, respectively. As we have highlighted in Proposition 2, the cost function restricted in the cell $\mathfrak{V}_i$ actually attains its minimum at the point $\bar{\mathrm{x}}_i^\star$, where, in general, $\bar{\mathrm{x}}_i^\star \neq \bar{\mathrm{x}}_i$ (the points $\bar{\mathrm{x}}_i^\star$ are denoted by red crosses in Fig. 2). The previous observation explains why in our simulations there exist generators $\bar{\mathrm{x}}_i \in \overline{\mathcal{X}}$ that are not interior points of their associated cells $\mathfrak{V}_i \in \mathfrak{V}$ in contradistinction with their corresponding points $\bar{\mathrm{x}}_i^\star \in \overline{\mathcal{X}}^\star$, which turn out to be interior points of the same cells. We also observe that the initial velocity vector $\bar{\mathrm{v}}_i \in \overline{\mathcal{V}}$ of the i-th vehicle emanating from $\bar{\mathrm{x}}_i \in \overline{\mathcal{X}}$ aims toward the point $\bar{\mathrm{x}}_i^\star \in \overline{\mathcal{X}}^\star$, and thus aims toward the cell $\mathfrak{V}_i \in \mathfrak{V}$ associated with the i-th vehicle.

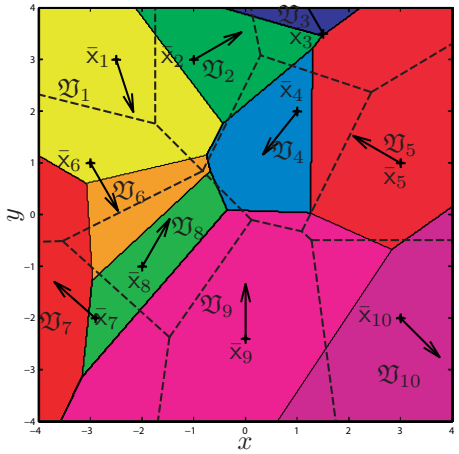

(a) The case when the weight $\varrho_i = 2$ for all $i \in \mathcal{I}_n$ (affine Voronoi diagram in $\mathbb{R}^2$).

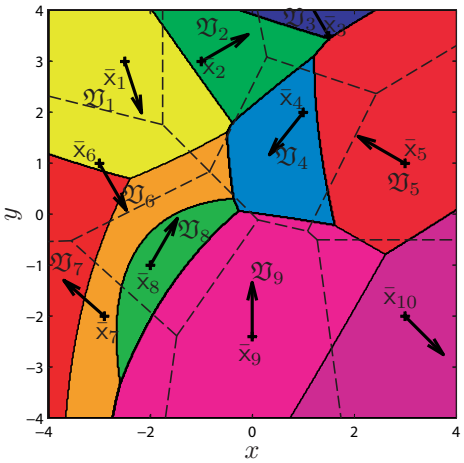

(b) The case when the weight $\varrho_i = i/5$ (restriction of a power Voronoi diagram in $\mathbb{R}^5$ to $\mathcal{X}(0)$).

Fig. 1. Generalized Voronoi diagrams generated by a set of ten points with respect to the minimum control effort.

6 Conclusion

We have proposed an area assignment problem for multi-vehicle systems, which we have framed as a generalized Voronoi diagram problem with respect to a state-dependent proximity metric. In particular, the proximity metric was taken to be the minimum square integral control (control effort) required for each vehicle to reach an arbitrary target point in the plane with a small terminal speed at a given terminal time. We have shown that the solution to this problem can be directly associated with a power Voronoi diagram in a higher dimensional Euclidean space. A notable feature of the problem here introduced has to do with the fact that the distribution of the weights attached to every possible direction of motion of each vehicle by means of the value function of the optimal control problem is not necessarily uniform. Consequently, each vehicle "prefers" to move along particular "less expensive" directions. A possible direction for future research is the extension of the techniques here introduced to more general classes of area assignment problems involving mechanical systems with nonlinear dynamics.

Acknowledgements

The author would like to thank the anonymous reviewers for their constructive comments and suggestions.

References

[1] A. Getis and B. Boots, *Models of Spatial Processes: An Approach to the Study of Point, Line and Area Patterns*. Cambridge, UK: Cambridge University Press, 1978.

[2] A. Okabe, B. Boots, K. Sugihara, and S. N. Chiu, *Spatial Tessellations: Concepts and Applications of Voronoi Diagrams*. West Sussex, England: John Wiley and Sons Ltd, second ed., 2000.

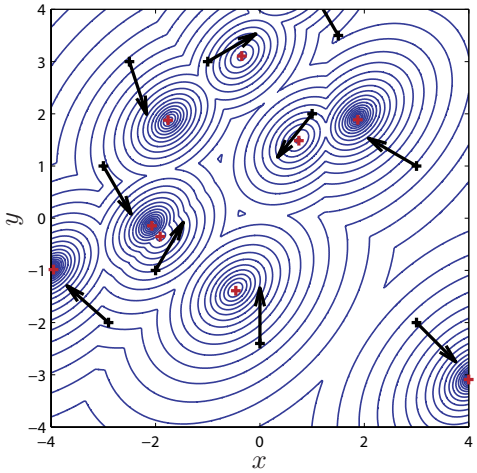

(a) The case when the weight $\varrho_i = 2$, for all $i \in \mathcal{I}_n$.

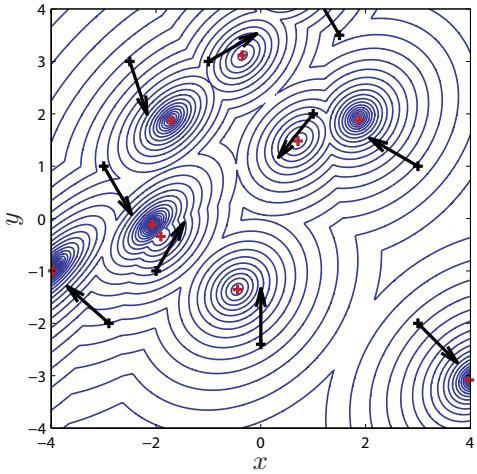

(b) The case when the weight $\varrho_i = i/5$, for $i \in \mathcal{I}_n$.

Fig. 2. Level sets of the lower envelope cost function $\underline{c}(\mathsf{x})$.

[3] F. Aurenhammer, "Voronoi diagrams: A survey of a fundamental geometric data structure," *ACM Computing Surveys*, vol. 23, no. 3, pp. 345–405, 1991.

[4] J.-D. Boissonnat and M. Yvinec, *Algorithmic Geometry*. Cambridge, United Kingdom: Cambridge University Press, 1998.

[5] J. Beasley and N. Christofides, "Vehicle routing with a sparse feasibility graph," *European Journal of Operational Research*, vol. 98, no. 3, pp. 499–511, 1997.

[6] F. Bullo, E. Frazzoli, M. Pavone, K. Savla, and S. Smith, "Dynamic vehicle routing for robotic systems," *Proceedings of the IEEE*, vol. 99, no. 9, pp. 1482–1504, 2010.

[7] M. Pavone, A. Arsie, E. Frazzoli, and F. Bullo, "Distributed algorithms for environment partitioning in mobile robotic networks," *IEEE Transactions on Automatic Control*, vol. 56, no. 8, pp. 1834–1848, 2011.

[8] J. Cortés, S. Martinez, T. Karatas, and F. Bullo, "Coverage control for mobile sensing networks," *IEEE Transactions on Robotics and Automation*, vol. 20, no. 2, pp. 243–255, 2004.

[9] A. Ghosh, "Estimating coverage holes and enhancing coverage in mixed sensor networks," in *29th IEEE Conference on Local Computer Networks*, pp. 68–76, Nov. 2004.

[10] S. Megerian, F. Koushanfar, M. Potkonjak, and M. Srivastava, "Worst and best-case coverage in sensor networks," *IEEE Transactions on Mobile Computing*, vol. 4, no. 1, pp. 84–92, 2005.

[11] J. Cortés, S. Martinez, and F. Bullo, "Spatially-distributed coverage optimization and control with limited-range interactions," *ESAIM: COCV*, vol. 11, no. 4, pp. 691–719, 2005.

[12] F. Labelle and J. R. Shewchuk, "Anisotropic Voronoi diagrams and guaranteed quality anisotropic mesh generation," in *SCG' 03*, pp. 191–200, 2003.

[13] A. Gusrialdi, S. Hirche, T. Hatanaka, and M. Fujita, "Voronoi based coverage control with anisotropic sensors," in *American Control Conference*, pp. 736–741, June 2008.

[14] E. Bakolas and P. Tsiotras, "The Zermelo-Voronoi diagram: a dynamic partition problem," *Automatica*, vol. 46, no. 12, pp. 2059–2067, 2010.

[15] E. Bakolas, Optimal steering for kinematic vehicles with applications to spatially distributed agents. Ph.D. dissertation, School of Aerospace Engineering, Georgia Institute of Technology, Atlanta, GA, 2011.

[16] E. Bakolas and P. Tsiotras, "Optimal partitioning for spatiotemporal coverage in a drift field," *Automatica*, vol. 49, no. 7, pp. 2064–2073, 2013.

[17] K. Sugihara, "Voronoi diagrams in a river," *International Journal of Computational Geometry and Applications*, vol. 2, no. 1, pp. 29–48, 1992.

[18] T. Nishida, K. Sugihara, and M. Kimura, "Stable marker-particle method for the Voronoi diagram in a flow field," *Journal of Computational and Applied Mathematics*, vol. 202, no. 2, pp. 377–391, 2007.

[19] A. E. Bryson and Y. C. Ho, *Applied Optimal Control*. Waltham, MA: Blaisdell Publication, 1969.

[20] M. Athans and P. L. Falb, *Optimal Control, An Introduction to the Theory and Its Applications*. New York: Dover Publications, 2007.

[21] P. Antsaklis and A. N. Michel, *Linear Systems*. Boston, MA: Birkhäuser, 2005.

[22] T. Basar and G. J. Olsder, *Dynamic Noncooperative Game Theory*. London: Academic Press, second ed., 1982.

[23] J.-D. Boissonnat, C. Wormser, and M. Yvinec, "Anisotropic diagrams: Labelle Shewchuk approach revisited," *Theoretical Computer Science*, vol. 408, no. 2–3, pp. 163–173, 2008.

[24] F. Aurenhammer, "Power diagrams: properties, algorithms and applications," *SIAM Journal on Computing*, vol. 16, no. 1, pp. 78–96, 1987.